U.S. ARMY

DEVCOM CHEMICAL BIOLOGICAL CENTER

U.S. ARMY COMBAT CAPABILITIES DEVELOPMENT COMMAND
CHEMICAL BIOLOGICAL CENTER
ABERDEEN PROVING GROUND, MD 21010-5424

DEVCOM CBC-TR-1854

Modeling Survival of *Bacillus anthracis* Spores Exposed to UVC and Simulated Solar Light

Thomas Ingersoll
Jana S. Kesavan
Vipin K. Rastogi

RESEARCH AND OPERATIONS DIRECTORATE

Daniel McGrady

Tech(X)
Aberdeen, Maryland 21001-3473

Jay Eversole

NAVAL RESEARCH LABORATORY
Washington, DC 20375-0001

Steven Hill

ARMY RESEARCH LABORATORY
Adelphi, MD 20783-1138

November 2023

Disclaimer

The findings in this report are not to be construed as an official Department of the Army position unless so designated by other authorizing documents.

REPORT DOCUMENTATION PAGE

1. REPORT DATE	2. REPORT TYPE	3. DATES COVERED	
		START DATE	END DATE
XX-11-2023	Final	Mar 2015	Dec 2017

4. TITLE AND SUBTITLE
Modeling Survival of *Bacillus anthracis* Spores Exposed to UVC and Simulated Solar Light

5a. CONTRACT NUMBER	5b. GRANT NUMBER	5c. PROGRAM ELEMENT NUMBER
CB10416		
5d. PROJECT NUMBER	**5e. TASK NUMBER**	**5f. WORK UNIT NUMBER**
CBCall14-AMD3-CBMV-01-2-0004		

6. AUTHOR(S)
Ingersoll, Thomas; Kesavan, Jana S.; Rastogi, Vipin K. (DEVCOM CBC); McGrady, Daniel (Tech(X)); Eversole, Jay (NRL); Hill, Steven (ARL)

7. PERFORMING ORGANIZATION NAME(S) AND ADDRESS(ES)
Director, DEVCOM CBC, ATTN: FCDD-CBR-IM, APG, MD 21010-5424
Tech(X) Corporation; 210 Research Boulevard, Suite 130, Aberdeen, MD 21001-3473
Naval Research Laboratory; 4555 Overlook Avenue SW, Washington, DC 20375-0001
DEVCOM ARL; 2800 Powder Mill Rd, Adelphi, MD 20783-1138

8. PERFORMING ORGANIZATION REPORT NUMBER
DEVCOM CBC-TR-1854

9. SPONSORING/MONITORING AGENCY NAME(S) AND ADDRESS(ES)	10. SPONSOR/MONITOR'S ACRONYM(S)	11. SPONSOR/MONITOR'S REPORT NUMBER(S)
Defense Threat Reduction Agency; 8725 John J. Kingman Road, MSC 6201, Fort Belvoir, VA 22060-6201	DTRA	

12. DISTRIBUTION/AVAILABILITY STATEMENT
Distribution Statement A. Approved for public release: distribution unlimited.

13. SUPPLEMENTARY NOTES

14. ABSTRACT
The effect of exposure to germicidal ultraviolet-C (UVC) and simulated solar light upon relative survival of *Bacillus anthracis* spores was measured across several experimental covariates, and corresponding statistical models were developed. These covariates included bacteria strain; Ames versus Sterne strain; UV versus simulated solar light; spore particle size; substrates including membrane filter, fiber, quartz slide, and aerosol; and the deposition method. A non-linear model, Annelis (1965), described loss of viability in response to light exposure and was supported over simpler models. The graphic model comparison method using confidence intervals was chosen for comparing covariate levels. The deposition method had an effect on variance but little effect on expected values. Confidence intervals broadly overlapped across the range of doses between most covariate levels, with the following noteworthy exceptions: small particles in aerosol and on quartz exhibited higher survival at low exposures than particles on fiber, Ames exhibited higher viability at low exposures than Sterne strain in small particles on quartz, quartz may be used as a proxy for aerosol in those conditions experimentation with aerosols is precluded, and higher survival in the pathogenic strain Ames should be accounted for when using non-pathogenic Sterne strain as a proxy in models.

15. SUBJECT TERMS

Germicidal ultraviolet-C (UVC)	Particle size	Aerosol
Non-linear model	*Bacillus anthracis* (Ba)	Viability
Ba Sterne strain	Ba Ames strain	

16. SECURITY CLASSIFICATION OF:			17. LIMITATION OF ABSTRACT	18. NUMBER OF PAGES
a. REPORT	b. ABSTRACT	C. THIS PAGE		
U	U	U	UU	42

19a. NAME OF RESPONSIBLE PERSON	19b. PHONE NUMBER *(Include area code)*
Renu B. Rastogi	(410) 436-7545

STANDARD FORM 298 (REV. 5/2020)
Prescribed by ANSI Std. Z39.18

Blank

PREFACE

The work described in this report was authorized under project no. CBCall14-AMD3-CBMV-01-2-0004. The work was started in March 2015 and completed in December 2017.

The use of either trade or manufacturers' names in this report does not constitute an official endorsement of any commercial products. This report may not be cited for purposes of advertisement.

This report has been approved for public release.

Acknowledgments

Research and development funding was provided by Defense Threat Reduction Agency (Fort Belvoir, VA). The authors extend appreciation to the following individuals from U.S. Army Combat Capabilities Development Command Chemical Biological Center (Aberdeen Proving Ground, MD) for their hard work and assistance with the execution of this technical program:

- Frank Handler (Retired),
- Aime Goad,
- Jerry Cabalo, and
- Michael Kierzewski.

Blank

CONTENTS

FIGURES

TABLES

Blank

MODELING SURVIVAL OF *BACILLUS ANTHRACIS* SPORES RESPONDING TO EXPOSURE TO LIGHT

1. INTRODUCTION

Statistical models were developed to provide predictive formulae describing relative survival of bacteria spores in response to light exposure under a suite of factorial covariates including species composition, cluster size, aerosol versus pipette deposition, and germicidal ultraviolet-C (UVC) versus simulated solar light exposures. Relative survival was measured as the fraction of viable spores with the ability to grow into colonies in subsequent culture. Exposure (fluence) was calculated by multiplying light intensity (flux) and exposure duration (time). Models, which describe relative survival in response to exposure, are based on established equations for decay curves (Annelis et al., 1965; Anderson and May, 1995). These models were developed from the Classical Shoulder Model (CSM; eq 1; Annelis et al., 1965).

$$S = 1 - \left(1 - \left(e^{-V*D}\right)\right)^N \quad (1)$$

Where S is the survival fraction, V is the decay constant, D is the normalized exposure (sample dose/maximum dose), e is the base of the natural logarithm, and N is the shoulder constant.

The presence of a shoulder in the survival curve suggests that spores can absorb some radiation without significant impact to survival and that survival is reduced only when some threshold of dose is attained. Annelis et al. (1965) discuss several factors, which could contribute to the shoulder and tail shape of decay curves produced in the CSM versus exponential decay for *Clostridium botulinum* spores; however, inadequate data were available to draw conclusions. Tailing in data was not explained by outliers in spore chemical composition or shielding by other spores, which suggests that tailing might be explained by multiple light-sensitive intracellular targets of heterogeneous radiotolerance (multi-hit modeling; Armitage and Doll, 1961).

Equation 1 has the property to simplify to the formula for the Exponential Decay Model (EDM; Anderson & May, 1995) when $N = 1$ (eq 2).

$$S = e^{-V*D} \quad (2)$$

This property allows the shoulder term to be compared with exponential decay using hypothesis tests (Section 3). Exponential decay can be interpreted as lacking in a threshold effect, and decay can be characterized by a constant halving rate with respect to dose because $-V$ is a constant.

$$S = 2 \xrightarrow{yields} D = \frac{ln2}{-V} \quad (3)$$

When decay follows eq 1, the halving rate is not constant (unless $N = 1$) and is dependent on the value of N (Section 4).

Because both equations have an underlaying exponential form, they are asymptotic by nature. That is, no non-zero level of exposure exists where survival is absolute and $S = 1$, even when a threshold is suggested by $N > 1$. Similarly, there are no finite levels of exposure resulting in complete extinction when $S = 0$; therefore, tailing is coerced by model formulae.

2. METHODS

Experimental design created a nested structure of factor levels: three levels of particle size (large, medium, and small or single spores), four levels of substrate (aerosol, quartz, filter, and fiber), two bacteria species (Sterne strain and Ames), and two levels of light source (simulated solar and UVC). However, data could not be collected for all the combination factors. For example, restrictions within Biosafety Level 3 (BSL-3) allowed only 1 µm particle data and no aerosol deposition to be collected for agent Ames. The net result is that 18 factor combinations were tested (Table 1). A model was developed for each factor combination and for comparisons between the levels, where relevant, to project goals (Table 2).

Table 1. Experimental Factor Level Combinations at which Data Were Collected

Light Source	Solar						UVC		
Agent	Sterne				Ames		Sterne		
Medium	Aerosol	Quartz	Filter	Fiber	Quartz	Filter	Aerosol	Quartz	Filter
Size (µm)	4				single spore	single spore	4		
	1	1	2.5 1	1			1	single spore	2.5 1

All models were implemented in R software (R Core Team (2019)) using non-linear modeling available in the R *stats* library function *nls* (Bates and Watts, 1988). Use of the non-linear least-squares algorithm required that starting values be approximated a priori to avoid convergence failure. A set of functions was written in R software that approximated starting values across a small set of user-supplied values. Those values produced the highest likelihood and were then used to initiate a more precise estimate of model coefficients using the R function *nls*. Selection between a shouldered model and a model of exponential decay was then performed using the R function *anova*.

Simulated solar light-intensity measurements were integrated across a spectrum of 280–400 nm. Across the study period, absolute intensity of solar simulation was found to vary by as much as 9% (Table 2) when measured in joules per meter squared seconds (J/m^2sec). Absolute intensity was then multiplied by exposure duration to determine the overall light dosage (flux) in joules per meter squared (J/m^2; Figures 1–19).

Table 2. Integrated Light Intensity across Wavelengths 280–400 nm

Integrated intensity (J/m^2sec)					
56.39	58.16	58.28	58.451	58.52	58.68
59.07	59.12	59.15	59.37	59.65	59.77
59.78	61.45	61.89	62.16	NA	NA

NA, not available.

3. RESULTS

3.1 Tabulated Models

A formal hypothesis test comparing CSM with EDM for the significance of the shoulder term was performed for all levels of light source, agent (Sterne versus Ames), and substrate (Table 3). Additional hypothesis tests (CSM versus EDM) were performed by nesting spore particle sizes within the above levels (Table 4). The shoulder term was found to be significant in most cases but not all (Section 4).

Table 3. Hypothesis Tests for Model Shape: Primary Models

Light Source	Agent	Substrate	Formula	Є ~	Shoulder Pr > F =
Solar	Sterne	Aerosol	$S = 1 - \left(1 - (e^{-10.7*D})\right)^{10.5} + Є$	$\mathcal{N}(0, 0.19)$	6.6 e-07
		Quartz	$S = 1 - \left(1 - (e^{-14.8*D})\right)^{17.8} + Є$	$\mathcal{N}(0, 0.25)$	8.7 e-09
		Filter	$S = e^{-3.8*D} + Є$	$\mathcal{N}(0, 0.17)$	0.5
		Fiber	$S = e^{-3.5*D} + Є$	$\mathcal{N}(0, 0.20)$	0.1
	Ames	Quartz	$S = 1 - \left(1 - (e^{-19.5*D})\right)^{671.2} + Є$	$\mathcal{N}(0, 0.08)$	2.2 e-16
		Filter	$S = e^{-4.7*D} + Є$	$\mathcal{N}(0, 0.14)$	0.8
UVC	Sterne	Aerosol	$S = 1 - \left(1 - (e^{-9.2*D})\right)^{3.2} + Є$	$\mathcal{N}(0, 0.21)$	7.5 e-3
		Quartz	$S = 1 - \left(1 - (e^{-8.8*D})\right)^{4.5} + Є$	$\mathcal{N}(0, 0.24)$	1.6 e-05
		Filter	$S = 1 - \left(1 - (e^{-11.5*D})\right)^{6.0} + Є$	$\mathcal{N}(0, 0.14)$	2.2 e-16

Table 4. Hypothesis Tests for Model Shape by Size

Light Source	Agent	Substrate	Size (μm)	Formula	Є ~	Shoulder Pr > F =
Solar	Sterne	Aerosol	4	$S = 1 - \left(1 - (e^{-7.2*D})\right)^{4.5} + Є$	$N(0, 0.18)$	2.9 e-04
			1	$S = 1 - \left(1 - (e^{-15.0*D})\right)^{29.5} + Є$	$N(0, 0.19)$	3.2 e-04
		Quartz	4	$S = 1 - \left(1 - (e^{-13.2*D})\right)^{14.6} + Є$	$N(0, 0.20)$	2.5 e-05
			1	$S = 1 - \left(1 - (e^{-15.9*D})\right)^{21.2} + Є$	$N(0, 0.27)$	3.6 e-05
		Filter	4	$S = e^{-4.5*D} + Є$	$N(0, 0.20)$	0.09
			2.5	$S = 1 - \left(1 - (e^{-6.8*D})\right)^{3.1} + Є$	$N(0, 0.08)$	2.8 e-08
			1	$S = e^{-3.7*D} + Є$	$N(0, 0.16)$	0.3
		Fiber	4	$S = 1 - \left(1 - (e^{-8.7*D})\right)^{6.0} + Є$	$N(0, 0.12)$	1.8 e-07
			1	$S = e^{-4.0*D} + Є$	$N(0, 0.20)$	0.1
UVC		Aerosol	4	$S = 1 - \left(1 - (e^{-7.0*D})\right)^{3.0} + Є$	$N(0, 0.08)$	6.6 e-05
			1	$S = 1 - \left(1 - (e^{-11.5*D})\right)^{4.7} + Є$	$N(0, 0.26)$	0.03
		Quartz	4	$S = e^{-2.4*D} + Є$	$N(0, 0.25)$	0.17
			1	$S = 1 - \left(1 - (e^{-10.2*D})\right)^{5.4} + Є$	$N(0, 0.24)$	2.5 e-05
		Filter	4	$S = 1 - \left(1 - (e^{-6.2*D})\right)^{4.6} + Є$	$N(0, 0.06)$	5.3 e-09
			2.5	$S = 1 - \left(1 - (e^{-18.4*D})\right)^{17.3} + Є$	$N(0, 0.06)$	5.1 e-12
			1	$S = 1 - \left(1 - (e^{-12.3*D})\right)^{6.2} + Є$	$N(0, 0.12)$	9.5 e-16

Model terms were tabulated for each experimental level (Table 5).

Table 5. CSMs by Experiment

Substrate	Sp.	Size (µm)	Method	Type	Model	Fig.
Filter	Sterne	1	Pipette	UVC	$S = 1 - \left(1 - (e^{-14.5*D})\right)^{14.3} + \mathcal{N}(0, 0.03)$	2
			Aerosol		$S = 1 - \left(1 - (e^{-14.2*D})\right)^{13.1} + \mathcal{N}(0, 0.06)$	
Filter		1	Pipette	Solar	$S = 1 - \left(1 - (e^{-9.1*D})\right)^{4.3} + \mathcal{N}(0, 0.13)$	1
			Aerosol		$S = 1 - \left(1 - (e^{-6.9*D})\right)^{1.8} + \mathcal{N}(0, 0.13)$	
Filter		2.5	Aerosol	UVC	$S = 1 - \left(1 - (e^{-18.4*D})\right)^{17.3} + \mathcal{N}(0, 0.06)$	5
		4			$S = 1 - \left(1 - (e^{-6.2*D})\right)^{4.6} + \mathcal{N}(0, 0.06)$	
		2.5		Solar	$S = 1 - \left(1 - (e^{-6.8*D})\right)^{3.1} + \mathcal{N}(0, 0.08)$	6
		4			$S = 1 - \left(1 - (e^{-2.8*D})\right)^{0.5} + \mathcal{N}(0, 0.20)$	
Quartz		1	Pipette	UVC	$S = 1 - \left(1 - (e^{-16.4*D})\right)^{10.6} + \mathcal{N}(0, 0.07)$	2
			Aerosol		$S = 1 - \left(1 - (e^{-6.2*D})\right)^{3.2} + \mathcal{N}(0, 0.30)9)$	
Quartz		1	Pipette	Solar	$S = 1 - \left(1 - (e^{-9.4*D})\right)^{4.3} + \mathcal{N}(0, 0.13)$	1
			Aerosol		$S = 1 - \left(1 - (e^{-31.9*D})\right)^{480.1} + \mathcal{N}(0, 0.35)$	
Quartz		4	Aerosol	UVC	$S = 1 - \left(1 - (e^{-5.7*D})\right)^{2.7} + \mathcal{N}(0, 0.24)$	8
				Solar	$S = 1 - \left(1 - (e^{-13.2*D})\right)^{14.6} + \mathcal{N}(0, 0.20)$	7
Syn. Fiber		1		Solar	$S = 1 - \left(1 - (e^{-2.0*D})\right)^{6.0} + \mathcal{N}(0, 0.20)$	9
		4			$S = 1 - \left(1 - (e^{-8.7*D})\right)^{0.5} + \mathcal{N}(0, 0.12)$	
Aerosol		1			$S = 1 - \left(1 - (e^{-15.0*D})\right)^{29.5} + \mathcal{N}(0, 0.19)$	3
		4			$S = 1 - \left(1 - (e^{-7.2*D})\right)^{4.5} + \mathcal{N}(0, 0.18)$	
		1		UVC	$S = 1 - \left(1 - (e^{-11.5*D})\right)^{4.7} + \mathcal{N}(0, 0.26)$	4
		4			$S = 1 - \left(1 - (e^{-7.0*D})\right)^{3.0} + \mathcal{N}(0, 0.08)$	
Quartz	Ames	1	Pipette	Solar	$S = 1 - \left(1 - (e^{-19.5*D})\right)^{671.2} + \mathcal{N}(0, 0.08)$	10
Filter					$S = 1 - \left(1 - (e^{-5.0*D})\right)^{1.1} + \mathcal{N}(0, 0.14)$	

Fig., figure.
Sp., species.
Syn., synthetic.

3.2 Graphical Comparisons

Because models were nonlinear, graphical comparisons demonstrated overlap between confidence intervals at different regions of the curve (Figure 1). Differences in main effects were therefore inferred for those regions where confidence intervals were non-overlapping.

Figure 1 shows pipetting versus deposition of aerosolized *Bacillus anthracis* (Ba) Sterne strain on to a surface using a controllable aerosol device (CAD). Quartz exhibited overlapping confidence intervals; therefore, they could not be distinguished. High variability was observed in the CAD samples. The deposition method showed little effect on filter.

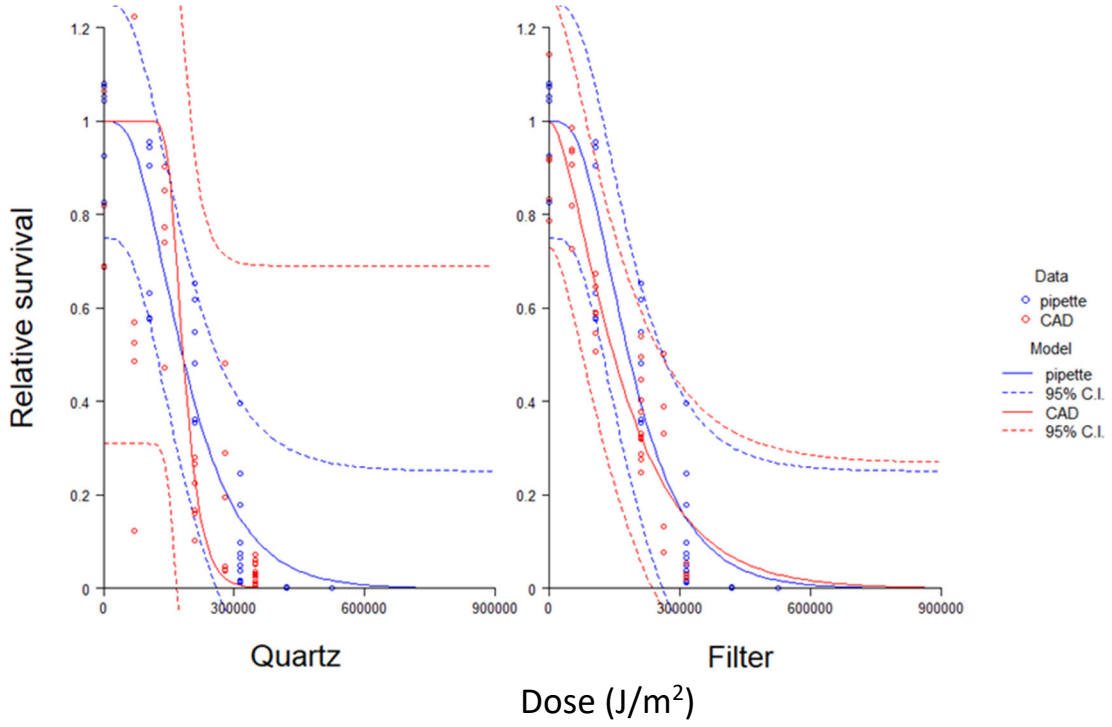

Figure 1. Comparison of deposition methods used for 1 µm particles of Ba Sterne strain on quartz and filter under simulated solar light.

Figure 2 shows relative survival fraction for 1 µm Ba Sterne strain deposited by pipetting and aerosol deposition via a CAD on a membrane filter and quartz slides and then exposed to UVC light. As with simulated solar light, differences in the responses on quartz to UVC exposure between the methods (i.e., pipette versus CAD) showed high variability in the CAD samples. The deposition method showed little effect when on filter. In all cases, confidence intervals overlapped.

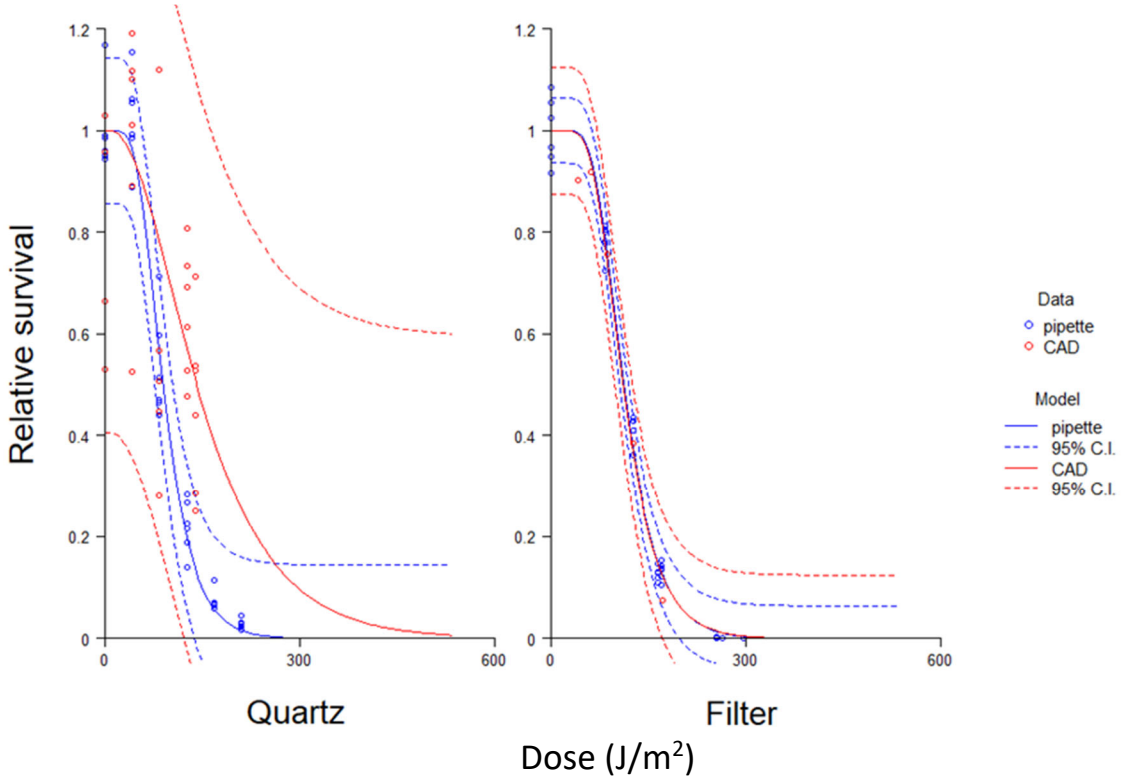

Figure 2. Comparison of deposition methods used for 1 µm particle of Ba Sterne strain on quartz and filter under UVC.

Figure 3 shows large and small sizes for strain Ba Sterne strain under simulated solar light in aerosols. Size showed little effect, which exhibited high variability and broad, overlapping confidence intervals.

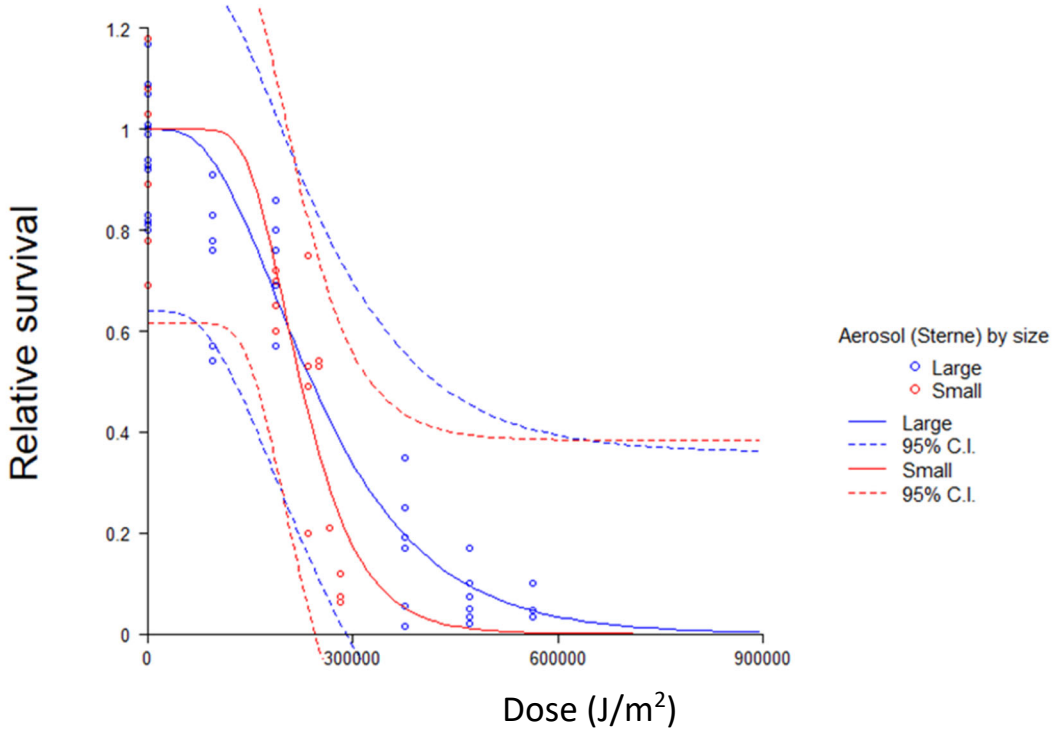

Figure 3. Effects of particle size Ba Sterne strain in aerosol under simulated solar light. Large (>40 spores/cluster) and small (<40 spores/cluster) particles.

Figure 4 compares aerosol sizes of Ba Sterne strain under UVC. Size had little effect on expected values (confidence intervals overlapped), but the small particles exhibited higher variability than the large ones.

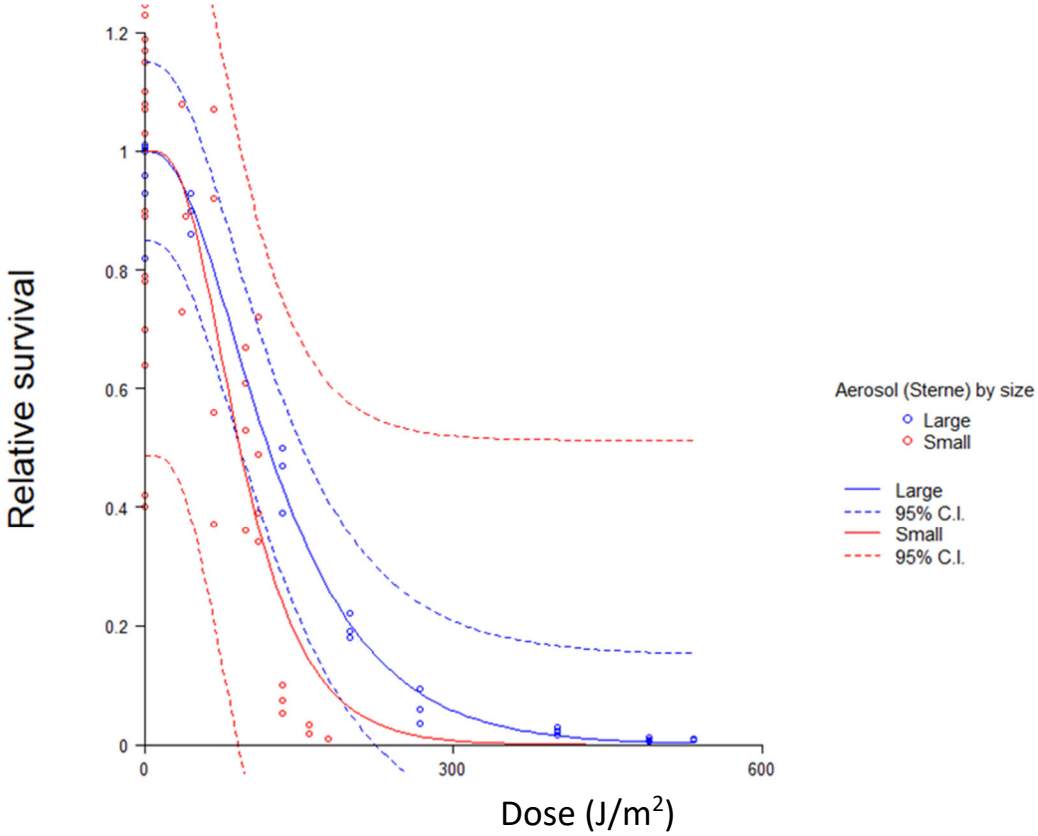

Figure 4. Effects of particle size Ba Sterne strain in aerosol under UVC. Small (<3 spores/cluster) and large (>40 spores/cluster) particles.

Figure 5 shows size and the deposition method for strain Ba Sterne strain on filter under UVC. Small and medium particles exhibited little difference regardless of the deposition method, while large particles exhibited higher survival across intermediate dosages (confidence intervals were regionally non-overlapping).

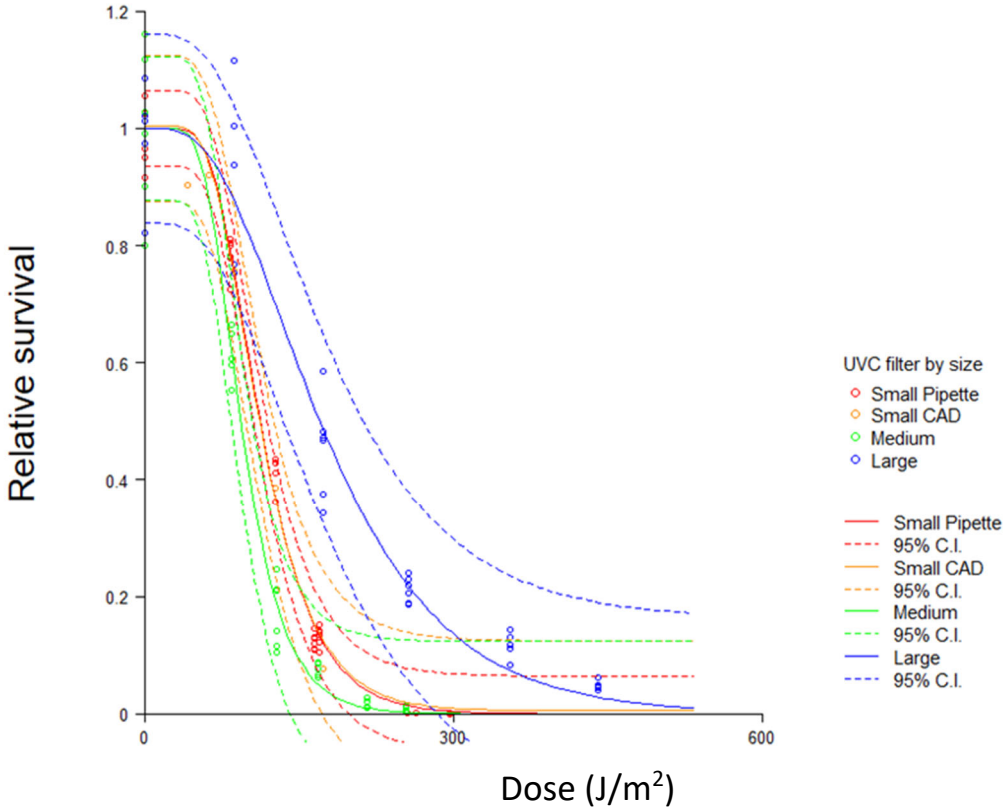

Figure 5. Effects of particle size and deposition method for Ba Sterne strain on filter under UVC. Small pipette/CAD (1 spore/cluster), medium (IJAG; 13–16 spores/cluster), and large (IJAG; 46–64 spores/cluster) particles.

In Figure 6, particle size and the deposition method for strain Ba Sterne strain on filter are compared. Variability was high in all cases except medium particles, resulting in little distinction between main effects (confidence intervals overlap).

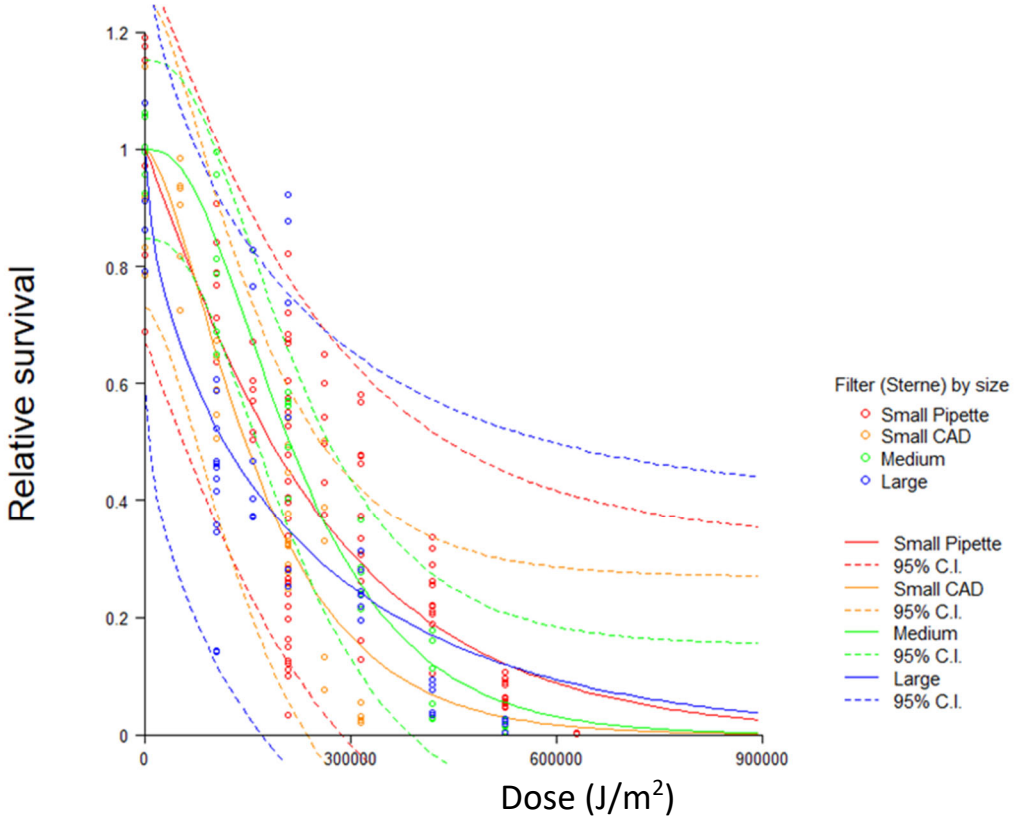

Figure 6. Effects of particle size and deposition method for Ba Sterne strain on filter under simulated solar light. Small pipette/CAD (1 spore/cluster), medium (IJAG; 13–16 spores/cluster), and large (IJAG; 46–64 spores/cluster).

Figure 7 shows particle size and the deposition method for strain Ba Sterne on quartz. Variability was very high for small particles generated by CAD and moderately high for large particles, with comparatively little distinction between main effects (the confidence intervals overlapped).

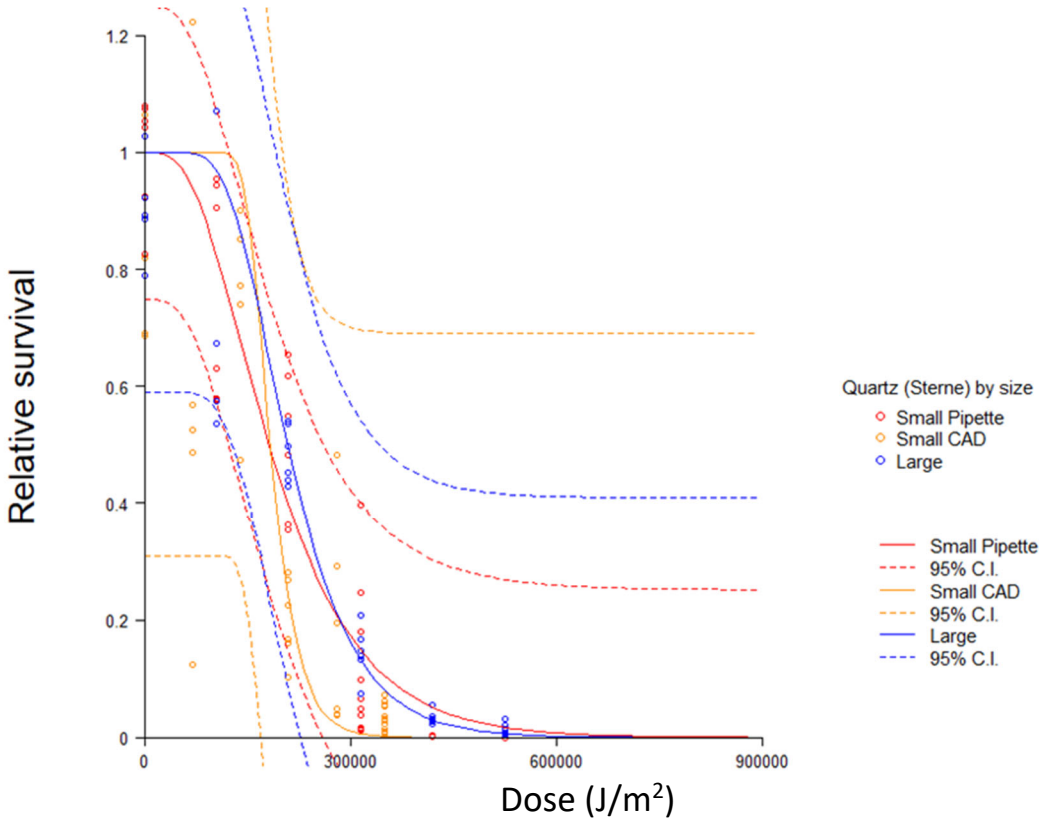

Figure 7. Effects of particle size and deposition method for Ba Sterne strain on quartz under simulated solar light. Small pipette/CAD (1 spore/cluster) and large (IJAG; >40 spores/cluster).

Figure 8 shows size and the deposition method for strain Ba Sterne strain on quartz. In all cases except small particles generated by pipette variability was high, resulting in insignificant differences between main effects (the confidence intervals overlapped).

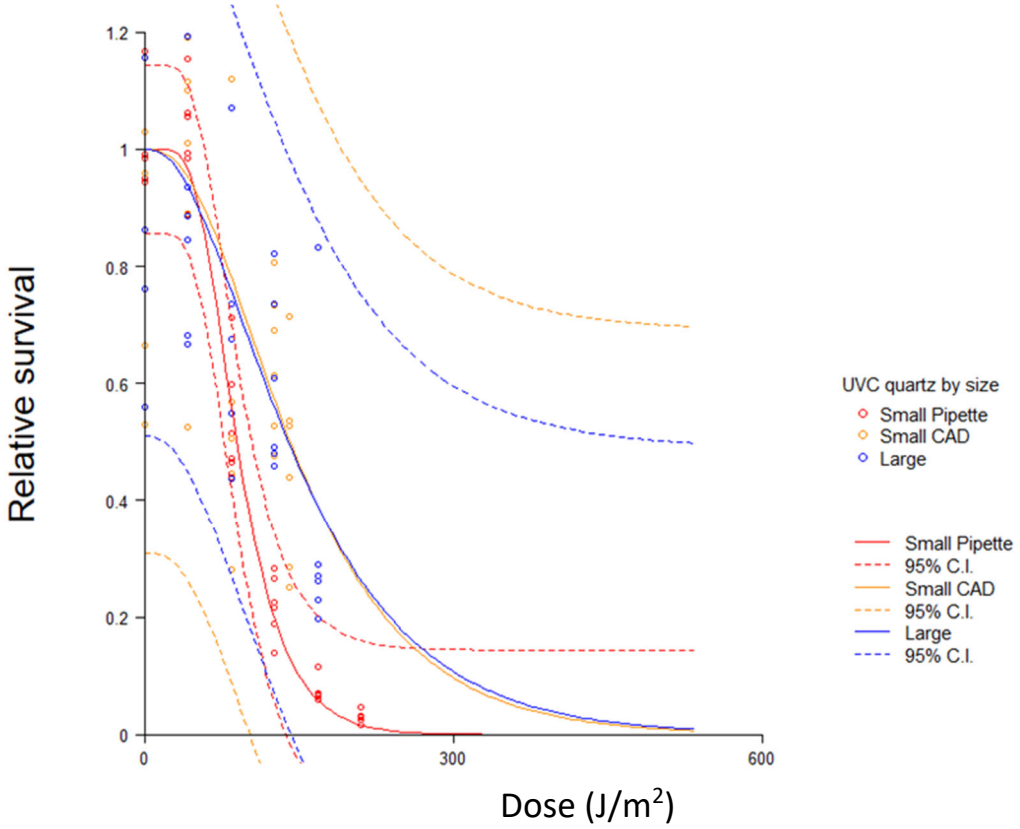

Figure 8. Effects of particle size and deposition method for Ba Sterne strain on quartz under UVC. Small pipette/CAD (single spores) and large (IJAG; >40 spores/cluster).

Figure 9 shows the size for strain Ba Sterne on fiber. In small particles variability was high rendering differences insignificant.

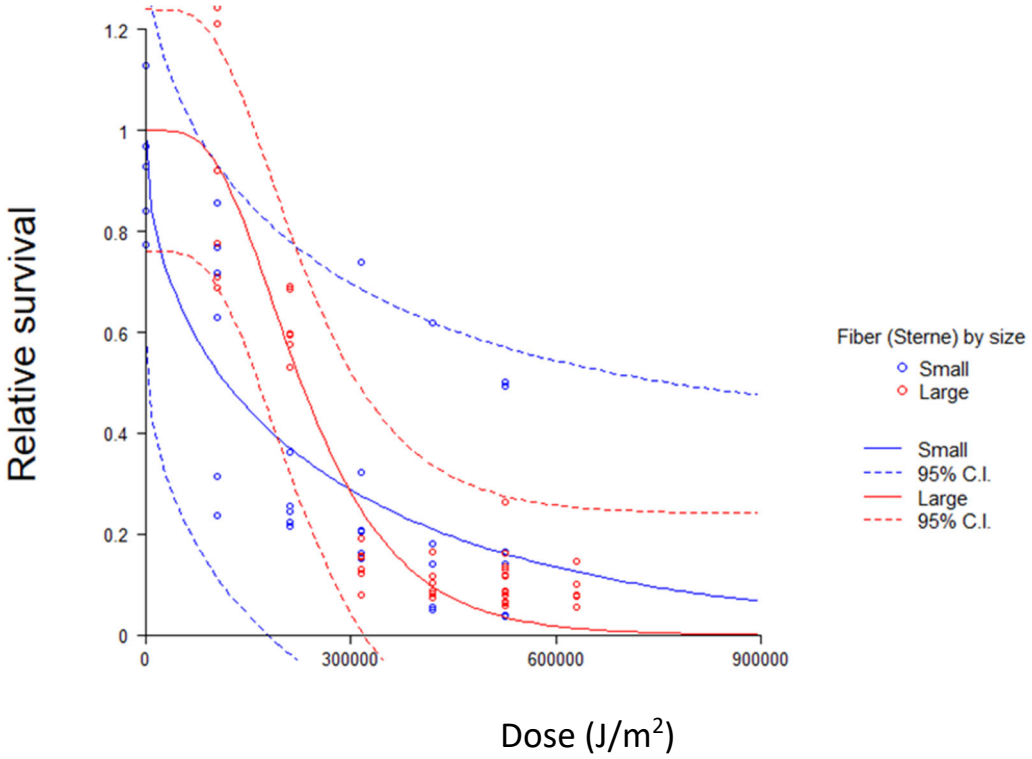

Figure 9. Effects of particle size for Ba Sterne strain on fiber under simulated solar light. Small (1 spore/cluster) and large (>30 spores/cluster).

Figure 10 shows the effect of media and quartz versus filter on Ba Ames strain. Particles on quartz exhibited higher survival at lower doses, below ~400000 Jm^2, than those on filter (non-overlapping confidence intervals).

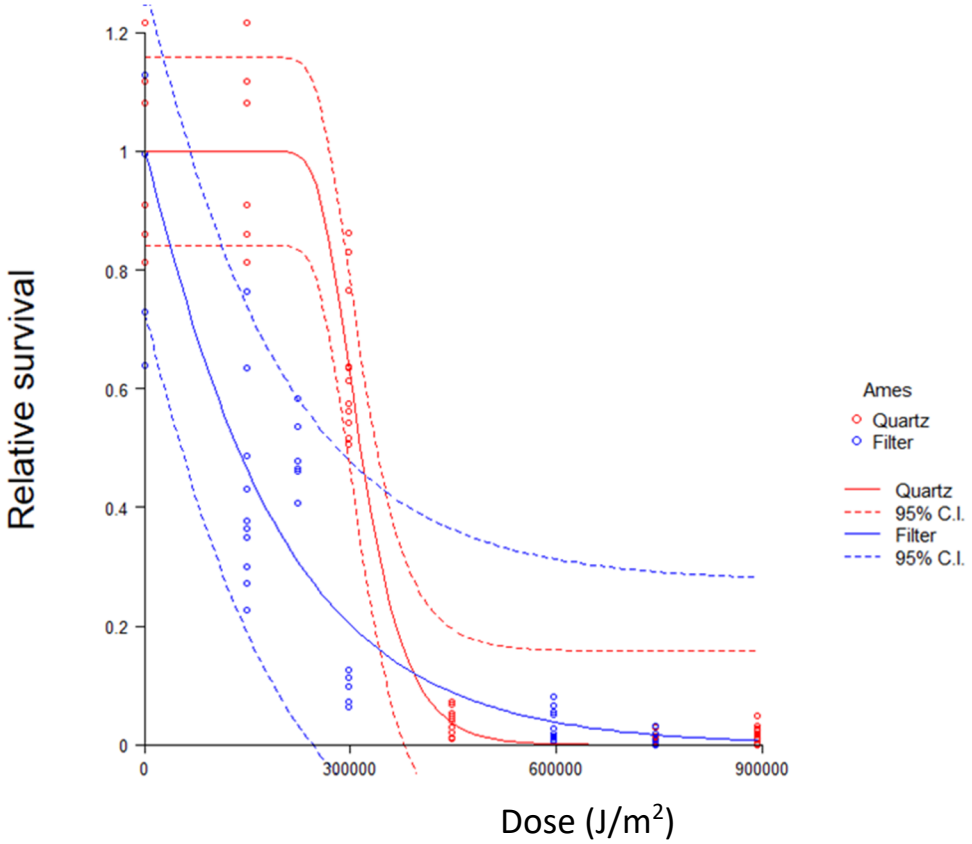

Figure 10. Effects on substrate of Ba Ames strain under simulated solar light.

Figure 11 shows the deposition method and substrate for strain Ba Sterne strain under simulated solar light. In most cases, variability was high. Confidence intervals overlapped.

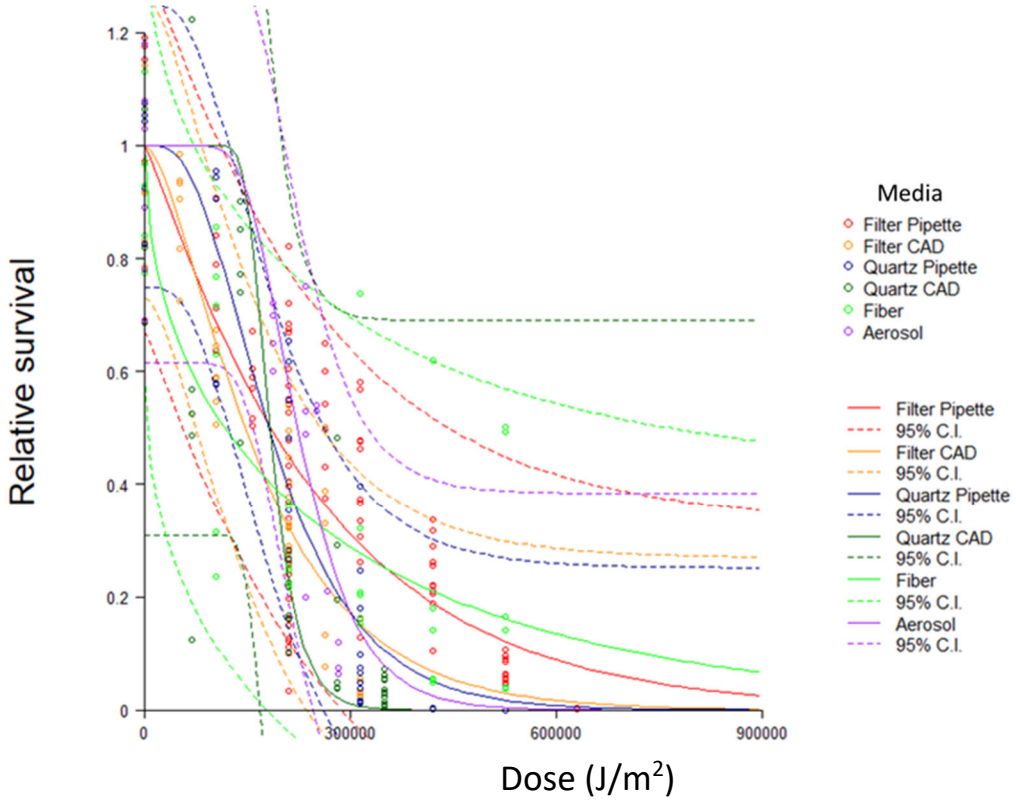

Figure 11. Effects of substrate and deposition methods for 1 µm particles of Ba Sterne strain under simulated solar light.

Figure 12 shows substrates for Ba Sterne strain under simulated solar light. Quartz, fiber, and aerosol exhibited similar responses with overlapping confidence intervals, while filter had lower survival at all but high doses.

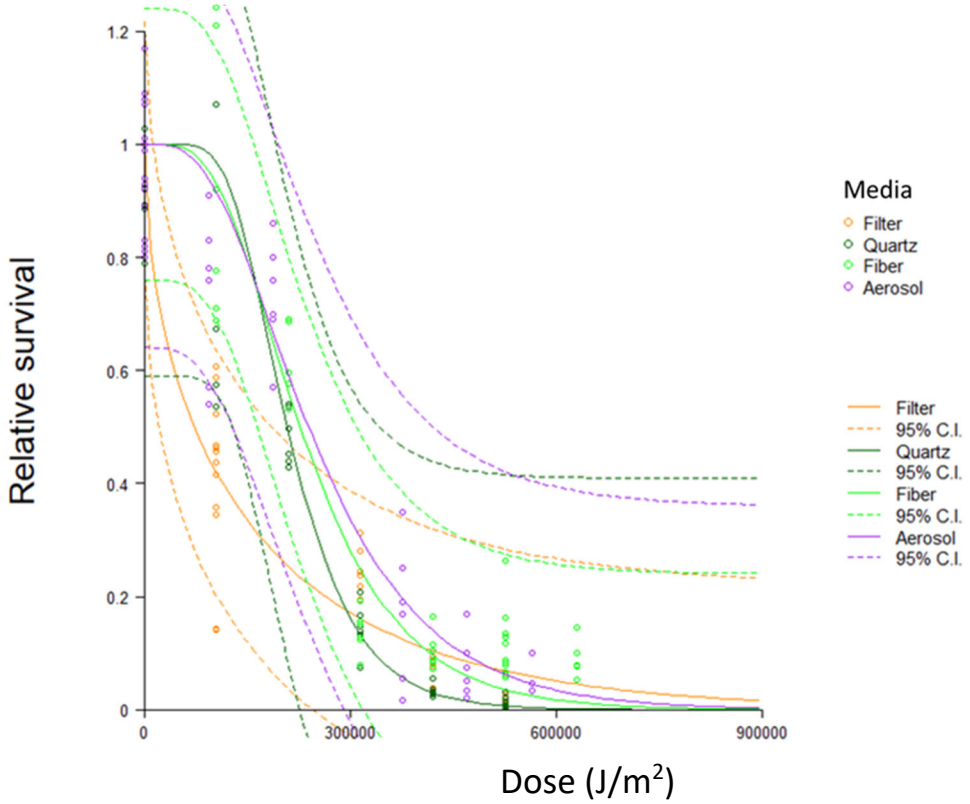

Figure 12. Effect of media in 4 µm particles of Ba Sterne strain under simulated solar light.

Figure 13 shows the deposition method and substrate for Ba Sterne strain under UVC. Quartz, CAD, and aerosol had higher variability. Confidence intervals overlapped.

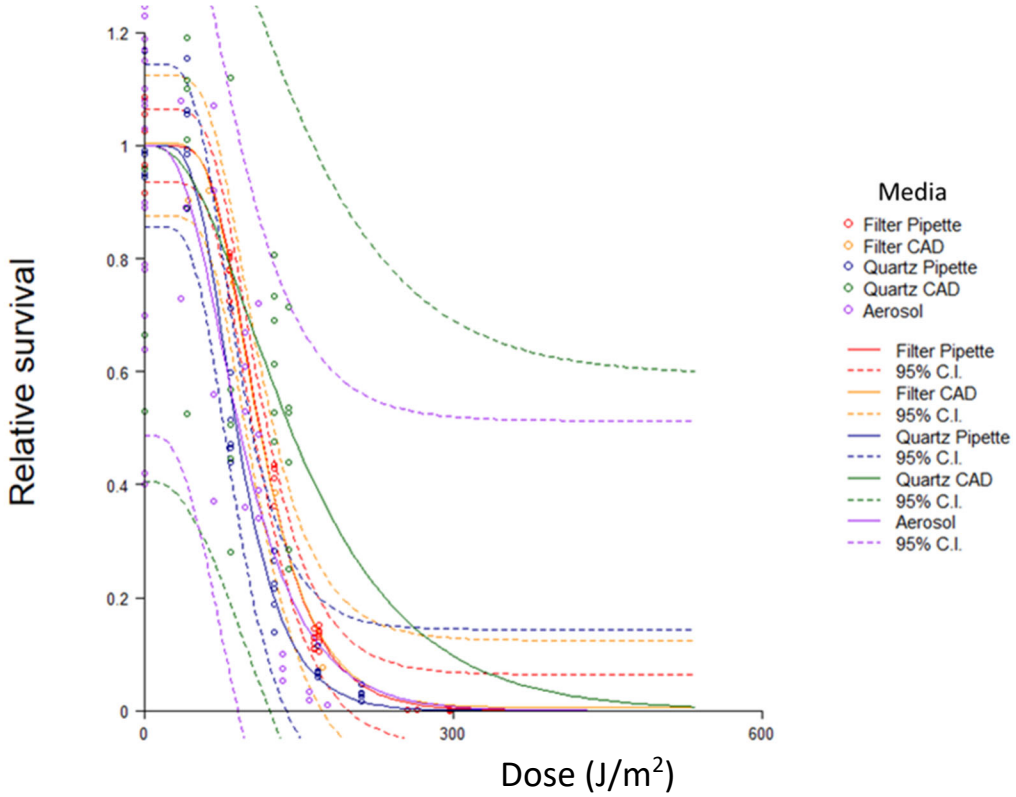

Figure 13. Effects of surface and deposition methods in 1 µm particles of Ba Sterne strain under UVC.

Figure 14 shows the effect of media for 4 µm particles of Ba Sterne strain under UVC. Confidence values overlapped, and quartz had higher variability.

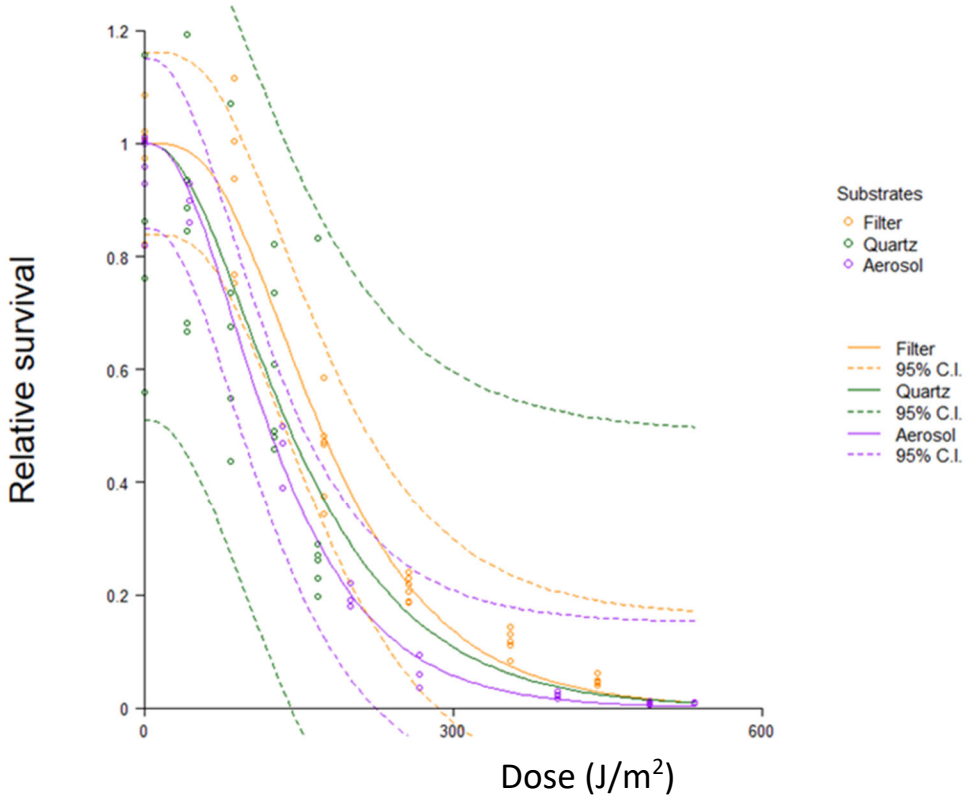

Figure 14. Effect of media in 4 µm particles of Ba Sterne strain under UVC.

Figure 15 shows Ba Ames and Ba Sterne strains pipetted on quartz and a filter under simulated solar light. Ba Ames strain on quartz exhibited higher survival at low to mid dosages (under ~40000 Jm^2) than Ba Sterne and Ba Ames strains on filter.

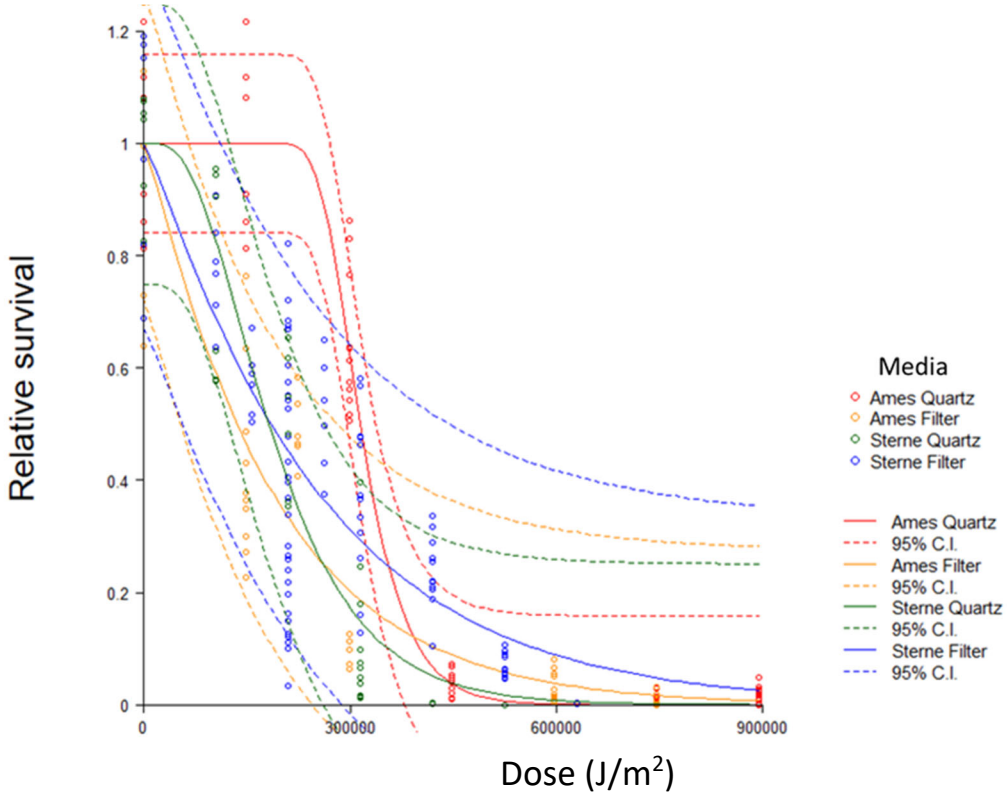

Figure 15. Effects of both strains on pipette-deposited quartz and filter substrates for 1 µm particles under simulated solar light.

Figure 16 shows Ba Ames strain deposited by pipette and Ba Sterne strain deposited by CAD on quartz and filter. Both Ba Ames and Ba Sterne strains on quartz had higher survival at low dosages (under ~20000 Jm^2) than that on filter. Ba Ames strain showed the highest survival up through ~40000 Jm^2 on quartz (non-overlapping confidence intervals). On filter, values were similar for both Ba Ames and Ba Sterne strains.

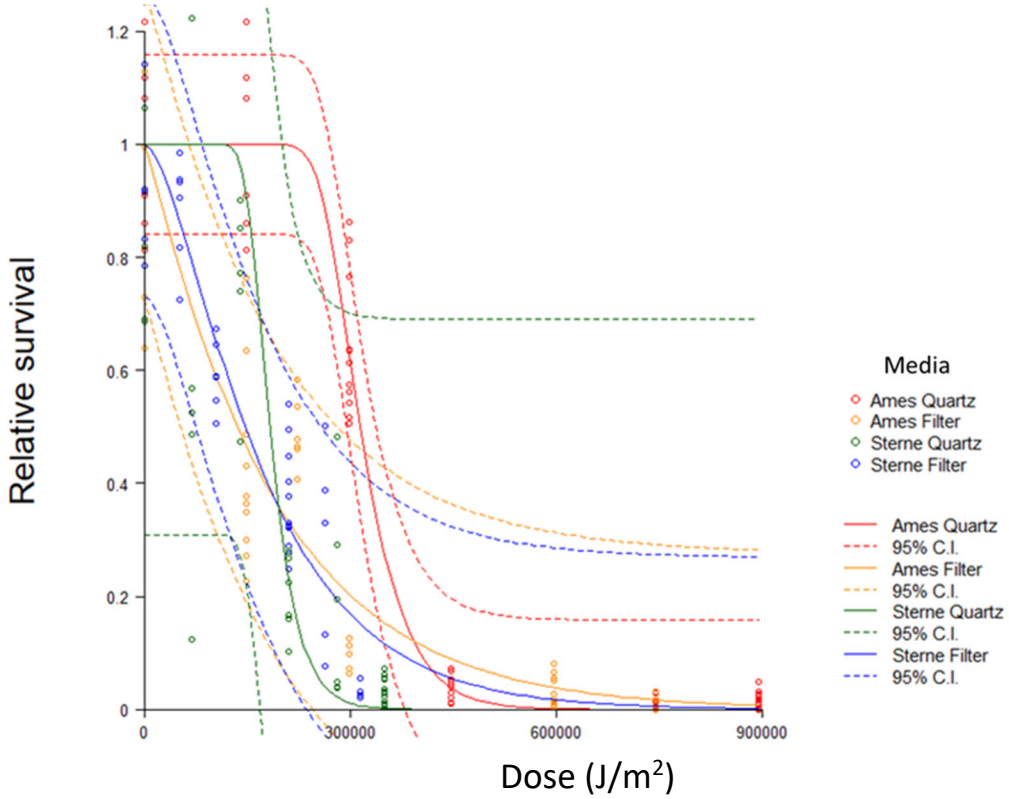

Figure 16. Effects of pipette-deposited Ba Ames and CAD-deposited Ba Sterne strains on quartz and filter surfaces for 1 μm particles under simulated solar light.

Figure 17 shows the effects of media category, transparent (17a) or opaque (17b), on quartz, aerosol, filter, and fiber by Ba Ames and Ba Sterne strains. Particles in aerosol or on quartz exhibited a clear shoulder, whereas those on filter and fiber exhibited exponential decay. The shoulder for Ba Ames strain was significantly longer than that of Sterne strain on quartz, suggesting that Ames strain is more resistant to low exposures of solar light than Sterne strain on a transparent quartz surface (non-overlapping confidence intervals). This was not the case on filter, where Sterne and Ames exhibited no significant differences (overlapping confidence intervals).

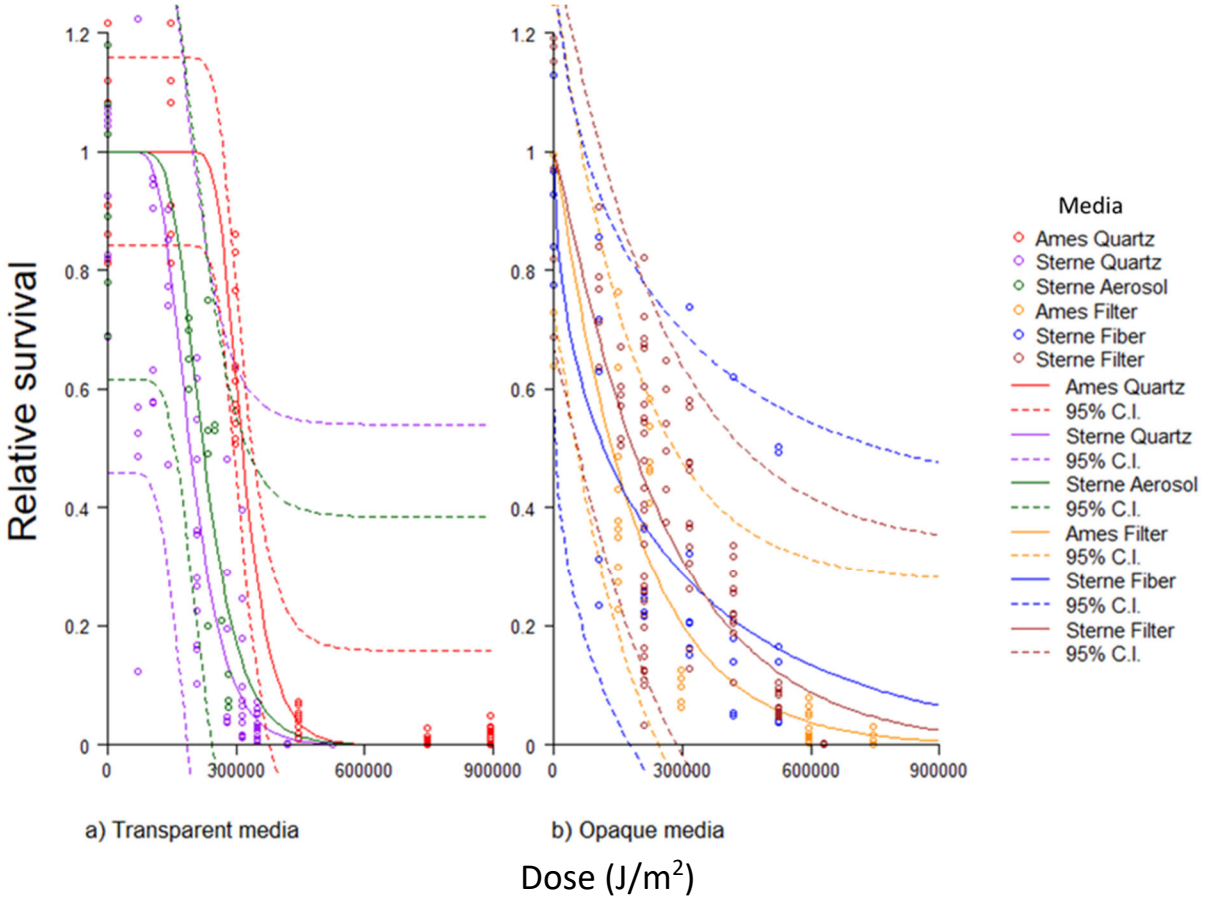

Figure 17. Similarities and differences of response curves grouped by media category for 1 µm particles under simulated solar light.

Figure 18 shows the effects of size and media for Ba Sterne strain on aerosol and filter. Confidence intervals broadly overlapped in all cases, although the expected value for small particles in aerosol extended slightly beyond the confidence interval for filter.

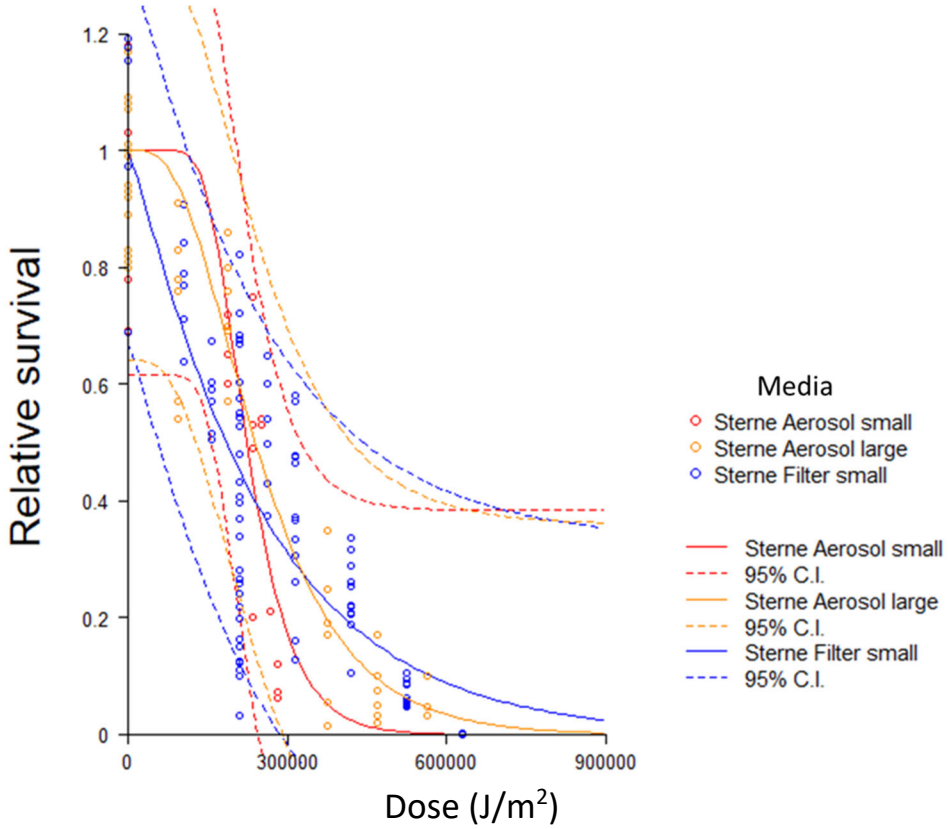

Figure 18. Effects of size and substrate for 1 µm Ba Sterne strain on filter vs large and small aerosol under simulated solar light.

Figure 19 shows the effects of size and media for Ba Sterne strain on quartz and filter. Confidence intervals broadly overlapped in all cases.

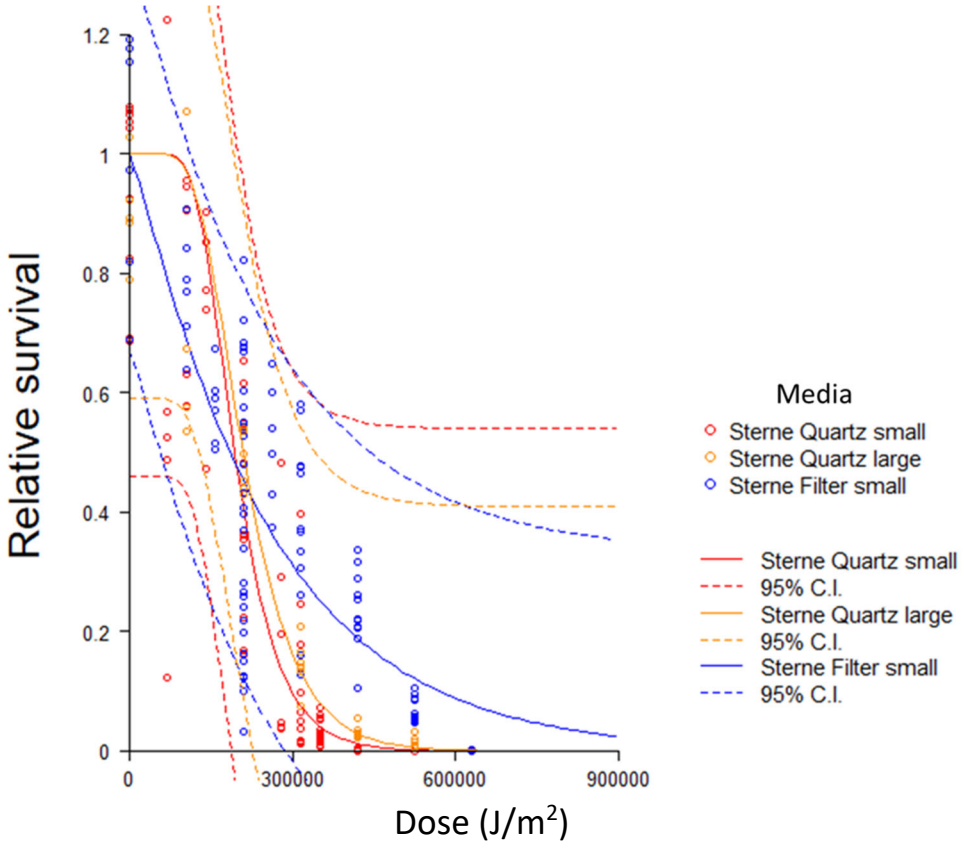

Figure 19. Effects of size and media for 1 µm Ba Sterne strain on filter vs large and small quartz under simulated solar light.

4. DISCUSSION

Formal hypothesis testing favored selection of a shouldered model in most cases (Table 3). Exceptions where a model of exponential decay was favored could largely be explained by high variance in the data or cases where the shoulder term was ~≤1. Because the shoulder model reduces to the exponential model by setting this term to 1, predictive models for cases where decay was approximately exponential were readily produced from the shoulder model (Table 4). When $N < 1$, decay at low doses is faster than exponential decay. When $N > 1$, decay at low doses is slower than exponential decay, thus shouldered. Therefore, eq 1 in which a constant halving rate is not implicit, provides a more generalized description of relative survival than the more restrictive eq 2.

An important, perhaps surprising consequence of the observed differences in N, is that small, aerosolized particles exhibit higher survival than large particles and particles on filters under low exposures (Figures 12 and 13). This suggests that small, aerosolized spore particles may survive across longer dispersal distances than expected when modeled against historic data.

A longer than expected dispersal distance has consequences for transport and dispersion modeling of aerosolized biological threats.

The deposition method had a strong effect on variability, with pipetting producing consistently narrower confidence intervals (Figures 1; 2). The effects of size were difficult to distinguish on filter (Figures 3 and 8) and somewhat difficult to distinguish on fiber (Figure 9). However, an interaction between size and substrate is apparent in aerosol, where small but not large particles exhibited higher survival in aerosol than on filter (Figure 18). Systematic sampling across these many experimental covariate levels was often precluded. For example, particle generation methods produced particle sizes that were clustered rather than continuous.

The non-pathogenic Ba Sterne strain has been proposed as a proxy for the highly pathogenic Ba Ames strain because it is safer and easier to work with. Ba Sterne strain might be used as a proxy under special conditions, but the relationship between the response curves of the two strains needs to be examined in more detail. The responses of both strains were very similar on filter, but Ba Ames strain had higher survival on quartz (Figure 17). Aerosol results are unavailable for Ames but in Sterne, aerosol and quartz responses were similar. An assumption that aerosol survival could be higher in Ames than in Sterne might therefore be reasonable, if unproven. In particular, viability of aerosolized Ba Ames strain particles transported in the environment may be underestimated by results obtained through the study of Sterne.

The preferred models (Table 4) could be used to produce computational simulations predicting agent survival for a range of conditions given the following caveats:

1) Data at very low and very high exposures are lacking. Models are less reliable at extreme values.

2) Data for many important environmental covariates such as temperature were available but not systematically sampled across ranges likely to be encountered in field conditions.

3) Restrictions imposed by experimental protocols such as those found in BSL3, and due to particle generation methods may have introduced confounding effects. For example, a continuous range of particle sizes could not be produced with current generation methods such as CAD.

4) Comparisons between the responses of Ba Sterne and Ames strains are marginally sufficient for modeling Ames on Sterne in special conditions found in our laboratory. However, environmental conditions may exist in the field that change the relationship between these response curves significantly.

Shouldered and exponential models are mathematically asymptotic on zero; therefore, both are tailed. Neither can describe complete extinction in a sample. However, to produce predictive models that include the probability of complete extinction, a stochastic model can be assembled by including a random term based on the reported variance (Table 4). This model can then be subjected to Monte Carlo sampling across multiple iterations to estimate extinction probabilities in response to light exposure.

LITERATURE CITED

1. Annelis, A.; Werkowski, S. Estimation of Radiation Resistance Values of Micro-organisms in Food Products. *Applied Microbiology* **1968,** 1300–1308.

2. Anderson, R.M.; May, M. *Infectious Diseases of Humans: Dynamics and Control*; Oxford Science Publications: Oxford, 1995.

3. Armitage, P.; Doll, R. Stochastic Models for Carcinogenesis. In *Proceedings of the Fourth Berkeley Symposium on Mathematical Statistics and Probability,* June 20–July 30, 1960; Statistical Laboratory of the University of California Press: Berkeley, CA, 1960.

4. R Core Team. R: A Language and Environment for Statistical Computing. R Foundation for Statistical Computing. Vienna, Austria, 2022. https://R-project.org (accessed 13 September 2023).

5. Bates, D.M.; Watts, D.G. *Nonlinear Regression Analysis and its Applications;* Wiley: New York, 1988.

Blank

ACRONYMS AND ABBREVIATIONS

BSL	Biosafety Level
CAD	controllable aerosol device
CSM	Classic Shoulder Model
EDM	Exponential Decay Model
Fig.	figure
J/m^2	joules per meter squared
J/m^2sec	joules per meter squared seconds
N/A	not available
Sp.	species
Syn.	synthetic
UVC	germicidal ultraviolet-C

DISTRIBUTION LIST

The following individuals and organizations were provided with one electronic version of this report:

U.S. Army Combat Capabilities
Development Command
Chemical Biological Center
(DEVCOM CBC)
FCDD-CBR-IM
ATTN: Ingersoll, T.
Kierzewski, M.

Defense Threat Reduction Agency
DTRA-RD-IAR
ATTN: Pate, B.

DEVCOM CBC Technical Library
FCDD-CBR-L
ATTN: Foppiano, S.
Stein, J.

Defense Technical Information Center
ATTN: DTIC OA

U.S. ARMY

U.S. ARMY COMBAT CAPABILITIES DEVELOPMENT COMMAND
CHEMICAL BIOLOGICAL CENTER